ELSEVIER

Journal of Nuclear Materials 296 (2001) 90–100

journal of nuclear materials

www.elsevier.com/locate/jnucmat

Section 3. Radiation effects

Multiscale modeling of radiation damage: applications to damage production by GeV proton irradiation of Cu and W, and pulsed irradiation effects in Cu and Fe

Maria Jose Caturla [a], Tomas Diaz de la Rubia [a], Maximo Victoria [b,*], R.K. Corzine [c], M.R. James [c], G.A. Greene [d]

[a] *University of California, Lawrence Livermore National Laboratory, Livermore, CA 94550, USA*
[b] *Swiss Federal Inst. of Technology-Centre of Research in Plasma Physics, Fusion Materials Technology Division, 5232 Villigen PSI, Switzerland*
[c] *Los Alamos National Laboratory, Los Alamos, NM 87545, USA*
[d] *Brookhaven National Laboratory, USA*

Abstract

The damage accumulation in Cu and W is investigated using a multiscale modeling approach. The efficiency for defect production of displacement cascades is calculated using molecular dynamics (MD). The simulation uses the recoil spectra from spallation reactions of 1.1 and 1.9 GeV protons as calculated with the Los Alamos High Energy Transport (LAHET) nuclear transport code. The total number of defects produced under these irradiation conditions is obtained both from the NRT and MD approximations. The value for the change in electrical resistivity produced by the irradiation-induced defect microstructure is compared to experimental values obtained from irradiations with protons of the above energies, showing a better agreement for the lower irradiation energy. The damage evolution is simulated with kinetic Monte Carlo, where the inputs for the calculation are the results from MD previously obtained. A large recovery of the damage is found at room temperature as a result of the migration of interstitial clusters, single vacancies and small vacancy clusters to sinks such as dislocations. Finally the effects of pulsed irradiation have been analyzed in Cu and Fe with similar simulation tools. The results indicate a clear influence of pulsing at 1 Hz, but not at higher frequencies.

1. Introduction

In the design of spallation neutron sources (SNS), beams of Gev protons, which are often pulsed, are used to produce neutrons with energies up to GeV. Thus, the materials in the target region of these devices are exposed to extremely aggressive irradiation environments. Moreover, depending on temperature, the pulse length may affect the material response. Assessing these effects is difficult since at present most of the information existing on radiation damage in materials is based on continuous fission reactor irradiation, where typical neutron energies are of the order of a few eV to a few MeV.

For GeV protons, the displacement damage is produced by the recoiling nucleus resultant from spallation nuclear reactions, which results also in the production of helium, neutrons and lower energy protons. Nuclear transport codes such as Los Alamos High Energy Transport (LAHET) are commonly used to obtain both the recoil spectra and the damage energy for a given irradiation condition. From these, one can then calculate displacement cross-sections by use of an appropriate relation between the number of defects produced and the damage. Accuracy of these models is crucial for predicting the damage level under these high energy irradiation conditions.

The conversion between damage energy and number of displacements produced is normally done using the

* Corresponding author. Tel.: +41-56 310 2063; fax: +41-56 310 4529.
E-mail address: max.victoria@psi.ch (M. Victoria).

0022-3115/01/$ - see front matter
PII: S0022-3115(01)00569-4

modified Kinchin–Pease model, also called NRT model [1]. However, during the past decade molecular dynamics (MD) simulations have shown that the total number of defects produced at recoil energies higher than a few keV is smaller than those predicted by the NRT model. Simulations in Fe and Cu, as well as in many other metals, have shown that the efficiency converges to a mean value of approximately 0.2–0.4 [2,3,13]. This, together with experiments carried out in the late 1970s by Averback and others, indicates that in order to calculate properly the number of defects produced by any given recoil, the intracascade recombination has to be taken into account [3].

In an effort to test the accuracy of the LAHET code at high energies, experiments have been performed at Brookhaven National Laboratory, in collaboration with Los Alamos National Laboratory, of proton irradiation at GeV energies of copper and tungsten wires. Electrical resistivity was measured at different dose levels. The results of these experiments can be used to test the models at high energies.

In this study we have calculated the change in resistivity using the most accurate models available, and compare the results with experimental observations. In order to compare the NRT and MD results we first computed the defects produced at different recoil energies using MD, and extracted the cascade efficiency with respect to the Kinchin–Pease model. These results are presented in Section 2. Next, recoil spectra for the conditions of the experiment were obtained using LAHET and the total defect production for these recoil spectra was computed both for the NRT model and using the results of MD simulations, as presented in Section 3. The final values of the resistivities so simulated are compared to the experimental measurements in Section 4. We have also studied the evolution of the damage produced in copper as a function of time at room temperature using a kinetic Monte Carlo (KMC) model, as shown in Section 5.

In order to investigate the possible effect of pulsing, we have carried out KMC simulations of damage accumulation in Fe at 1, 10, and 100 Hz for recoil spectra equivalent to 14 MeV neutrons. While the energy conditions are not identical to those for GeV protons described above, the results, presented in Section 6 provide some preliminary indication of the regimes in which pulse length effects may be important. More work clearly remains to be done on this problem. Finally we present a discussion of the results and conclusions.

2. Molecular dynamics simulations

2.1. Simulation setup

We have used molecular dynamics to study the damage produced by self-irradiation of copper, iron, and tungsten for energies up to 100 keV. For the case of copper the EAM interatomic potential [5] was used while for the case of iron and tungsten we used the interatomic potential developed by Finnis and Sinclair [6]. All potentials were smoothly fitted to the Universal potential [7] for short-range interactions. The system sizes used depended on the energy of the recoils, with the largest systems containing approximately 0.5 million atoms, and total simulation times ranging from 20 to 90 ps. For all the simulations periodic boundary conditions were used. The simulations were performed at 10 K and the simulation box was coupled to a thermal bath using Langevin dynamics in order to extract the temperature deposited by the energetic recoils. These calculations were done using the parallel code MDCASK. The performance of the code as a function of the number of processors and for different system sizes is shown in Fig. 1. The code has perfect scaling with the number of nodes for large systems. Simulations were performed both on the Cray T3E from Lawrence Berkeley National Laboratory and the IBM SP2 ASCI Blue at Lawrence Livermore National Laboratory.

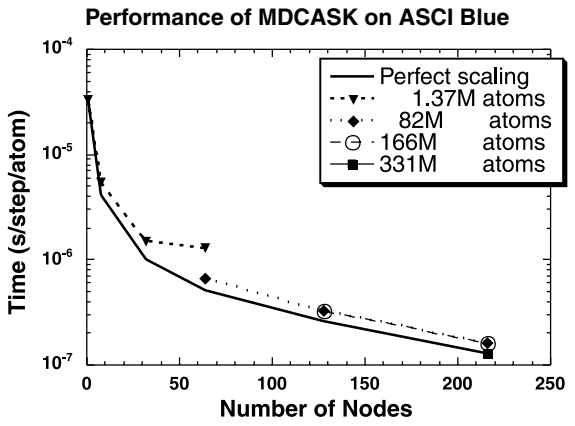

Fig. 1. Performance of MDCASK on ASCI blue.

2.2. Results

We have calculated the number of vacancies, interstitials and replacements produced in copper and tungsten for self-irradiation at energies between 200 eV and 100 keV. The MD results for iron have been published earlier [2,4,13] and will not be discussed here. The tables below show the results of these calculations for copper (Table 1(a)) and tungsten (Table 1(b)). This table includes the total number of cases for each energy, the average number of Frenkel pairs produced at each energy and the cascade efficiency, η. The cascade efficiency is defined as the number of Frenkel pairs obtained from the MD simulations at the end of the collision cascade, N_{MD}, divided by the number of Frenkel pairs derived

Table 1
Defects obtained from molecular dynamics simulations for different recoil energies

Energy (eV)	Number of MD runs	Average number of Frenkel pairs, N_{MD}	Frenkel pairs from NRT, N_{NRT}	Cascade efficiency, η
(a) In copper				
200	5	1.4	2	0.70
500	6	4.6	5	0.92
2000	5	13.4	20	0.67
5000	4	13.7	50	0.27
10000	3	21.0	100	0.21
20000	12	58.2	200	0.29
(b) In tungsten				
1000	3	4	4	1.0
2000	5	6	9	0.7
5000	5	8	22	0.4
10000	3	9	44	0.2
20000	3	18	89	0.2
30000	1	37	133	0.3
50000	2	43	222	0.2
100000	2	139	694	0.2

from the NRT model [1], $N_{NRT} = 0.8^{*}E_D/2E_d$, where E_D is the damage energy and E_d is the threshold displacement energy. Values of $E_d = 30$ eV and 90 eV for copper and tungsten, respectively, have been used for these calculations. The damage energy corresponds to the energy of the molecular dynamics simulations, since electronic energy losses are not included in these simulations. As observed in previous calculations [2–4], the cascade efficiency decreases as the energy increases, and reaches an asymptotic value of ~0.2 for high-energy recoils, as shown in Fig. 2. It is interesting to note that for both copper (Fig. 2(a)) and tungsten (Fig. 2(b)) the efficiency converges to the same value for high-energy recoils. This has been observed in simulations of damage in Fe [2,6] and other metals such as gold, vanadium, aluminum and nickel. The solid line in Fig. 3 represents a fit to the curves for cascade efficiency. The resulting fits are

$$\eta = 0.00228^{*}E_D + 0.7066^{*}E_D^{-0.437} \quad \text{for copper,}$$

$$\eta = 0.00506^{*}E_D + 1.0184^{*}E_D^{-0.667} \quad \text{for tungsten,}$$

where E_D is in keV.

We have fitted the total number of Frenkel pairs obtained from these simulations to a power law, in the same fashion as Bacon et al. [8]. The values obtained from these fits were $N_{MD} = 5.713^{*}E_D^{0.703}$ for Cu and $N_{MD} = 3.335^{*}E_D^{0.602}$ for W. These values are in agreement with those found by Bacon et al. [8].

We have analyzed in detail the morphology of the damage produced by these cascades, and the production of vacancy and interstitial clusters. In particular, one of the 20 keV copper cascades resulted in an interstitial cluster containing 38 defects that migrated along the

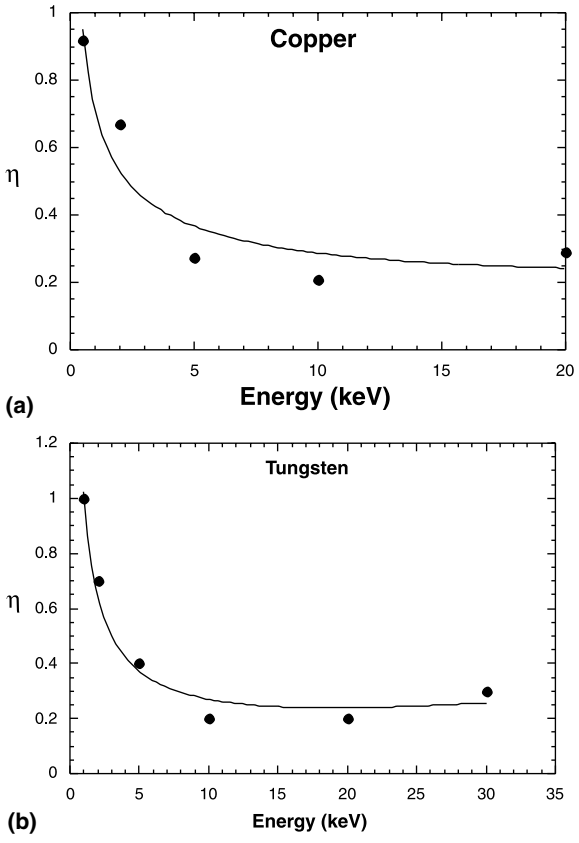

Fig. 2. Cascade efficiency for copper (a) and tungsten (b) as a function of recoil energy.

⟨1 1 0⟩ direction for times up to 89 ps at room temperature. Interestingly enough, due to the 1D migration, this cluster did not interact with the vacancy cluster also

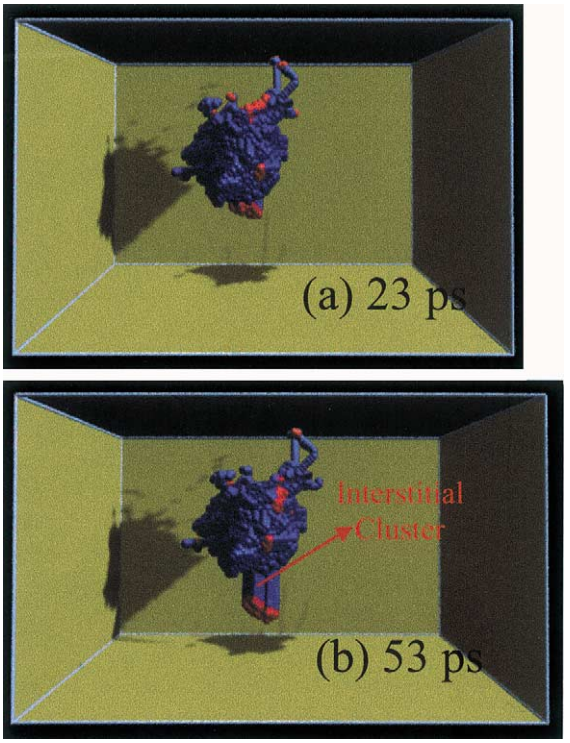

Fig. 3. Migration of an interstitial cluster produced in a copper cascade of 20 keV at (a) 23 ps and (b) 53 ps.

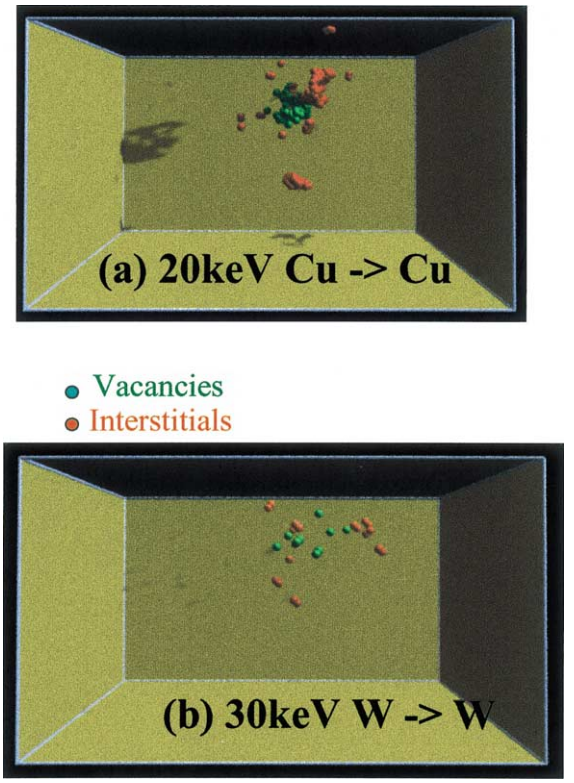

Fig. 4. Defect distribution after a cascade produced by (a) a 20 keV Cu recoil in Cu and (b) a 30 keV W recoil in W.

produced in the cascade. Fig. 3 shows the location of interstitials (in red) and replaced atoms (in blue) for this cascade and for two different times, 23 ps (Fig. 3(a)) and 53 ps (Fig. 3(b)). Observe the 1D migration and the fast diffusion. Detailed simulations of diffusivity of copper clusters by Osetsky et al. [9] have obtained values of migration energies for these interstitials of the order of ~0.4–0.08 eV. The migration of these clusters has important consequences for the final accumulated damage as we will show below.

Although the cascade efficiency is similar between copper, iron, and tungsten, the characteristics of the defect distribution are very different. While in copper most of the vacancies are forming clusters, in Fe and W vacancies are mainly isolated. This seems to be a characteristic of bcc materials, since the same behavior is seen in Fe [2,4]. Fig. 4 shows the results of a 20 keV Cu cascade (a) and a 30 keV tungsten cascade (b). Observe the lack of vacancy clustering in the tungsten case as opposed to the case of copper.

Using this MD-generated database we have obtained the cluster size distribution for vacancies and interstitials at different recoil energies. This study clearly shows that for any recoil energy, the amount of clustering of both vacancies and interstitials is larger in Cu than in W. In W the largest cluster contains only 12 defects for energies up to 100 keV, while in Cu clusters containing up to 50 defects have been observed for energies of 20 keV, and for both vacancies and interstitial type of defects. Fig. 5 shows the cluster size distribution for Cu (Figs. 5(a),(b)) and W (Figs. 5(c),(d)).

3. Damage due to GeV irradiation: recoil spectrum

The recoil spectrum for 1.1 and 1.94 GeV proton irradiation in copper and tungsten has been calculated by K. Corzine at LANL for the particular geometry of the experiment we are analyzing. In this case three wires were irradiated, two of copper and one of tungsten, which we will call Cu-1, Cu-2 and W, following their location with respect to the proton beam, with Cu-1 being the closest and W the furthest from the beam. Fig. 6 shows the recoil spectrum for 1.1 GeV irradiation (a) and 1.94 GeV irradiation (b). For this calculation a wire of length 3.582 cm and radius 2.54×10^{-3} cm^3 was used. As can be observed in Fig. 6, due to the small size of the samples, most of the protons travel through the samples without producing any damage, therefore the number of recoils per proton at any given energy is very small.

The deposited energy by all the recoils can also be obtained from these calculations, that is the total energy

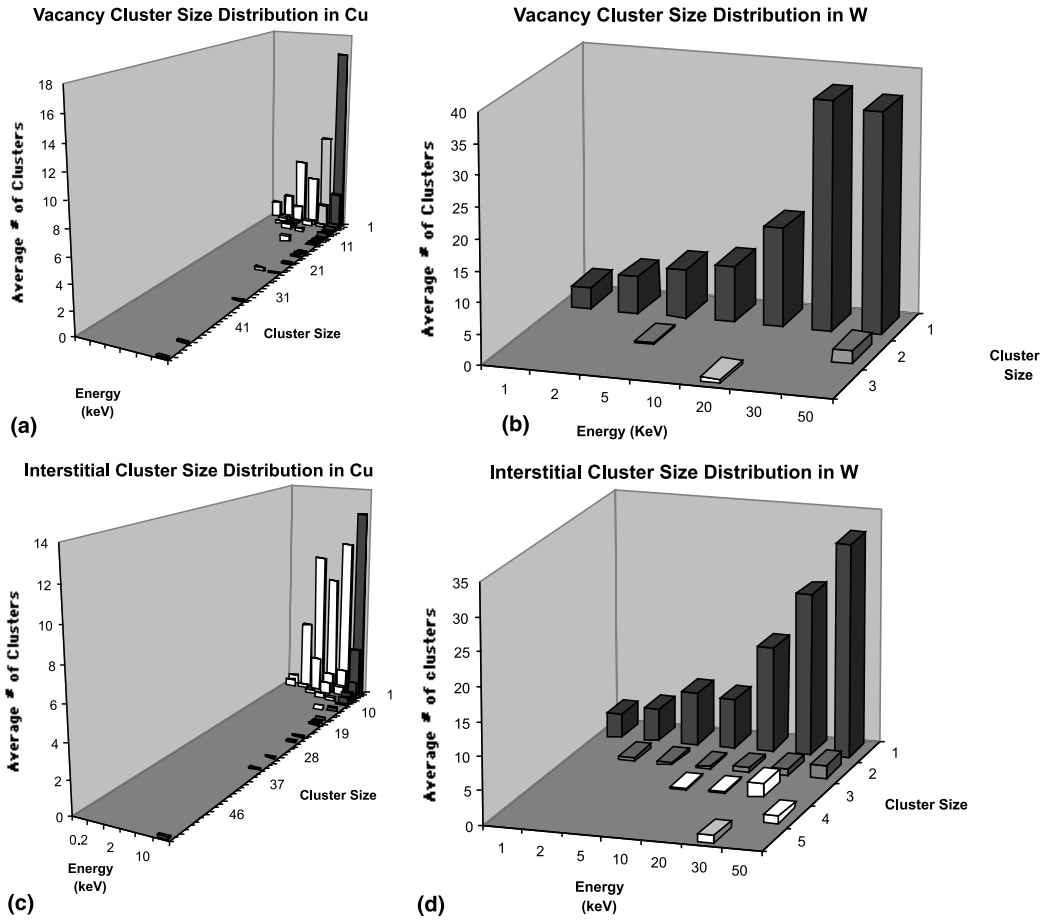

Fig. 5. Cluster size distribution for vacancies (a) and interstitials (b) produced by recoils of energies between 200 eV and 20 keV of Cu in Cu, and for vacancies (c) and interstitials (d) produced by recoils of energies between 1 and 50 keV of W in W.

that will result into structural damage on the irradiated sample. From the damage energy and using the NRT model it is possible to extract the total number of Frenkel pairs produced as a function of the recoil energy. These values are shown as circles in Fig. 7 for the case of 1.94 GeV in Cu (a) and tungsten (b). In the same figure, and represented by squares, we show the number of defects produced when the results of MD simulations are employed. In order to compute the number of defects from the MD simulations we have used the fits to the cascade efficiency shown in Fig. 2. In order to do this we had to assume a value for cascade efficiency for energies higher than 30 keV for copper and 100 keV for tungsten. A fixed value of 0.24 was used for the case of copper and 0.26 for the case of tungsten, corresponding to the value of the fit at the highest MD energy calculated. This approximation, which has been used by Stoller and Greenwood [10] to compute the damage in fission reactor pressure vessels due to neutron irradiations, is based on the concept of subcascade formation at high energies and should be rather robust for the conditions described here. As an example, in our calculations we have clearly observed subcascade formation in W at 50 keV, and others have observed subcascade formation in Fe at similar energies [2,4].

Integrating over the curves in Fig. 7 we can obtain the total number of Frenkel pairs produced per incoming proton, and considering the geometry of the system employed in the calculation we can obtain the displacement cross-section from the NRT model and the MD simulations. As expected, the cascade efficiency for copper and tungsten is 0.24 and 0.26, respectively, both for 1.1 and 1.94 GeV proton energies. That is, the correction in the NRT model is independent of energy for these high proton energies.

4. Comparison to experiments

Experiments were performed in Brookhaven National Laboratory in collaboration with Los Alamos National Laboratory to obtain the resistivity of Cu and

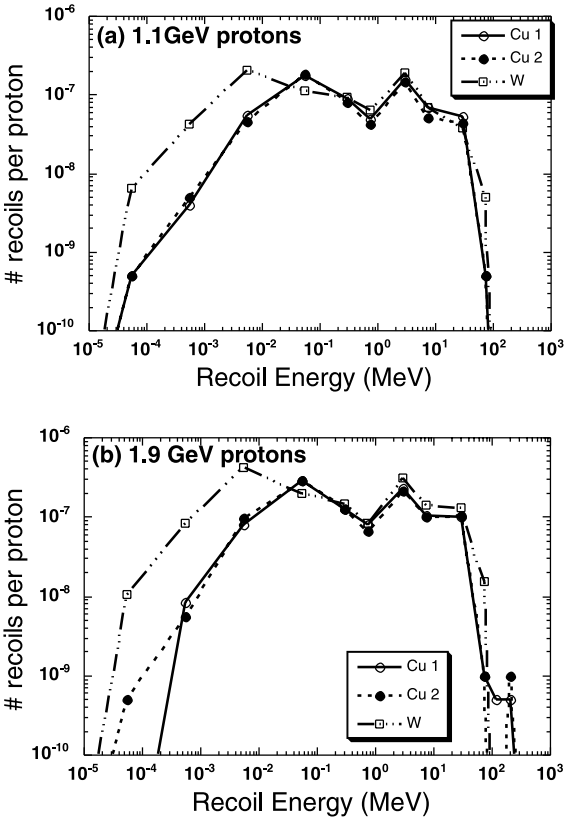

Fig. 6. Recoil spectrum for the case of 1.1 GeV (a) and 1.94 GeV (b) proton irradiation as calculated with LAHET.

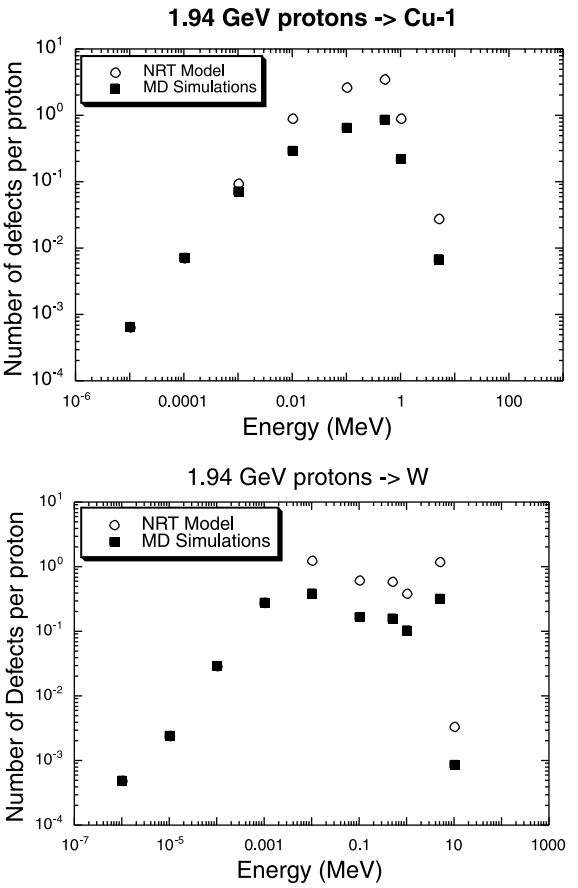

Fig. 7. Damage as calculated from the NRT model and from MD simulations for the case of 1.94 GeV proton irradiation of Cu-1 (a) sample and (b) tungsten.

W at different radiation doses and energies. The goal of these experiments was to test the damage cross-sections calculated with simulations codes such as LAHET at high energies.

In these experiments thin wires of Cu and W were irradiated with protons at two different energies, 1.10 and 1.94 GeV. Experiments were done at Liquid Helium temperature. Resistance was measured after irradiation at different doses. Two different copper samples and a tungsten sample were irradiated in the same experiment.

Solid dots on Figs. 8(a) and (b) show the results of the change in resistivity obtained from these experiments for the case of the first copper wire (Cu-1) and the tungsten wire, respectively.

These changes in resistivity, $\Delta\rho$, for different doses, Φ, and energies, E, can be calculated as

$$\Delta\rho(\Phi, E) = \Phi\sigma(E)\rho_{\mathrm{FP}}, \tag{1}$$

where $\sigma(E)$ is the displacement cross-section for energy E and ρ_{FP} is the resistivity change per Frenkel pair.

Two main components need to be checked in this expression to prove its validity:

1. value of the resistivity per Frenkel pair,
2. displacement cross-section.

The displacement cross-section is usually calculated from the damage energy obtained from codes such as LAHET and the NRT model for defect production, according to which, the number of defects as a function of the damage energy, E_{D} is

$$N_{\mathrm{NRT}} = 0.8^{*}E_{\mathrm{D}}/(2^{*}E_{\mathrm{th}}),$$

where E_{th} is the threshold displacement energy.

Using this approximation, damage cross-sections obtained from LAHET by Greene et al. [11], and resistivity per Frenkel pair values obtained from experiments for the case of Cu and estimated values for the case of tungsten, the change in resistivity is calculated for the conditions of the experiment. It should be noted that given the small fluences under consideration, the resistivity contribution from a very small quantity of spallation products has not been taken into account. These values are plotted as open circles in Fig. 8 for

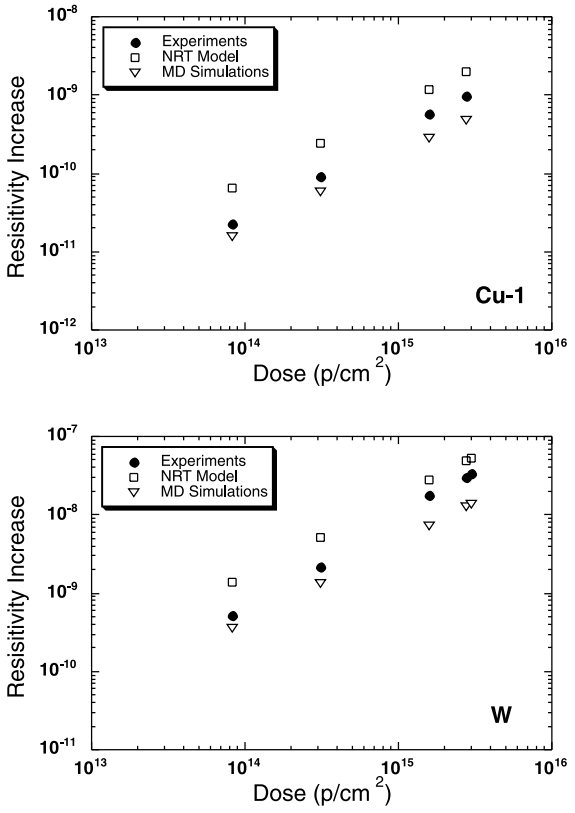

Fig. 8. Changes in resistivity as measured experimentally (solid dots) and calculated by the NRT model (open circles) and MD simulations (open squares) for the case of the (a) first copper wire, (b) second copper wire and (c) tungsten wire.

the two wires. The figure shows how the values calculated using the NRT model for defect production overestimates the resistivity values measured experimentally.

Many assumptions are included in the above relationship, (1). On one hand the resistivity per Frenkel pair must be known for the material in question. Accurate values for the resistivity increase due to Frenkel pairs in copper which are available in the literature, however that is not the case for tungsten. But besides the values of the resistivities there is an assumption implied in (1), that is, the resistivity is proportional to the number of Frenkel pairs produced. This is the final resistivity change is the sum of the resistivity per Frenkel pair, and that this change is the same for an isolated vacancy or a vacancy in a cluster. This point was addressed by Martin [12]. His calculations showed that this is a good approximation. We will assume this is the case for the analysis of the results presented in this report.

Using the correction coefficients to the NRT expression that we obtained from MD simulations, as explained in Section 2.2, we have calculated the change in resistivity for copper and tungsten from a modified displacement cross-section, that now includes the results from MD. The results are shown in Fig. 8 as open squares. From these figures we can see that there is good agreement of the simulation results with the experimental data for the lower energy, namely 1.1 GeV. However, there is a consistent larger discrepancy between the calculated and the experimental values for the case of 1.94 GeV.

In order to avoid the uncertainties in the value of change in resistivity per Frenkel pair for W and Cu, we have calculated the ratio between the measured resistivity changes at two different doses and energies for the same material. In this case:

$$\Delta\rho_{\exp}(\Phi,E)/\Delta\rho_{\exp}(\Phi\acute{1},E)=\Phi\sigma(E)/\Phi\acute{1}\sigma(E\acute{1}).$$

This ratio is independent of the assumed Frenkel pair resistivity which depends only on the ratio between displacement cross-sections. The left-hand side of this equation will be called the *measured ratio* and the right-hand side the *calculated ratio*. We use the experimental data provided by G. Greene and M. James to calculate the *measured ratios*, and the displacement cross-sections provided by Greene et al. [11] to obtain the *calculated ratios*. For the case of copper the *measured ratios* are 0.73–0.77 times the *calculated ratios* while for the case of W the *measured ratios* are 0.59–0.68 times the *calculated ratios*. This analysis provides us with some information about the validity of Eq. (1) and of the calculated displacement cross-sections. If the energy dependence is only given by the displacement cross-section, this dependence is not correctly reproduced by the calculations, being offset by approximately 0.7 for copper and 0.6 for W with respect to the experimental data. This discrepancy in the calculated displacement cross-sections could be due to:

(a) the calculated deposited energy by LAHET,
(b) the calculated number of defects from the NRT model.

The validity of the NRT model has been studied using MD simulations. From this analysis we observed that there is a factor of $\sim$0.24 for copper and $\sim$0.26 for W in the number of defects calculated from the NRT model and MD simulations. However this correction is independent of the energy of the protons, for the case of the high-energy protons in these experiments, as explained in Section 3. Therefore, we can conclude that the discrepancy between the experimental measurements and the calculations is related to the values of deposited energy computed by LAHET. It seems from this analysis that LAHET is underestimating the deposited energy for the case of 1.94 GeV while it gives an accurate value for the case of 1.1 GeV.

5. Damage evolution at room temperature

The evolution of the defects produced during the irradiation can be followed using a kinetic Monte Carlo simulation, with input from molecular dynamics. In these simulations we used a cube of 200 nm on each axis. In this box we included the damage produced by 1.9 GeV protons at a dose of 2.77×10^{15} protons/cm^2, conditions used experimentally. The distribution of this damage was done using the results from molecular dynamics simulations for different recoil energies. The number of cascades for each energy was taken for the recoil spectra calculated by K. Corzine at LANL.

These simulations show how the damage decreases as a function of time. Most of the recovery is produced at very short times, due to recombination of vacancies with fast diffusing interstitial clusters. These clusters move in one dimension and have migration energies of ~0.1 eV. Values for migration energies of vacancies and interstitial clusters and binding energies of clusters were obtained from experiments and MD simulations as described in earlier publications [4,13].

The average vacancy cluster size is constant in time, and ~25 defects per cluster, corresponding to a cluster size of ~1.5 nm. This is in agreement with TEM measurements of defects produced in copper by neutron irradiation [14]. The average size of interstitial clusters increases with time. This different behavior is due to the rapid migration of interstitial clusters. These interstitials can find other interstitial clusters and therefore cluster growth. Vacancy clusters, however, can only increase in size due to the aggregation of single vacancies or small vacancy clusters, up to size 4.

The processes occurring at this temperature are:

1. Interstitial clusters migrate to dislocations or other sinks, reducing the defect population. Some of these interstitials can recombine with single vacancies or vacancy clusters reducing also the total defect population.
2. Vacancies of sizes up to 4 also migrate. Some of them will recombine with interstitials (decrease of damage) while others will recombine with existing vacancy clusters.
3. Vacancy clusters do not dissociate at this temperature; therefore their concentration is mostly constant as a function of time. Observe that stage V in copper is at ~400 K.

The evolution of these defects in time is shown in Fig. 9. From these simulations we observe that in just 1 s at room temperature, the population of defects decreases 25%, that is 25% of the damage is recovered. This recovery is mostly due to loss of interstitial clusters to sinks and the recombination of vacancies with mobile interstitials. However, vacancy clusters will still remain in the system even after long annealing times. Extrapolating these results to longer times, the recovery after a few months would be of the order of 50%. This is in agreement with the experimental results where they see a large recovery of the damage in irradiated samples stored at room temperature.

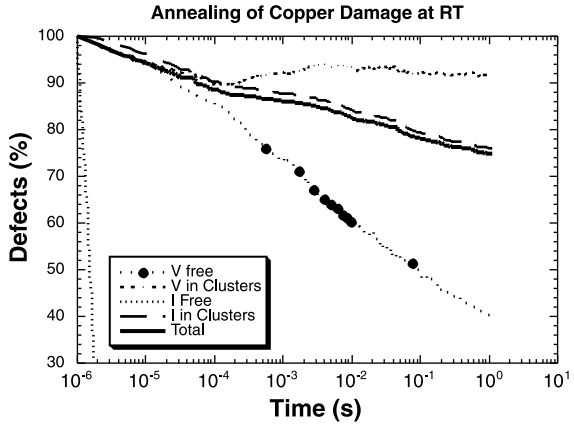

Fig. 9. Evolution of the damage in copper at room temperature in terms of percentage of defects with respect to the initial value after irradiation. Black line is the total number of defects.

6. Effect of pulsed irradiation on damage accumulation

Under most conditions, such as those that would be present in a magnetic fusion energy (MFE) plant, or when bombarding with fission neutrons, irradiation takes place at a certain dose rate and temperature, but in a continuous manner. However, in most spallation neutron sources, in an inertial fusion energy (IFE) reactor, or when using a pulsed neutron source such as that recently proposed by Perkins [15], the irradiation flux is pulsed and the interplay between temperature, flux, and pulse frequency controls the kinetics of damage accumulation. For sufficiently low pulse frequency, and at elevated temperature where defects migrate fast, it may be expected that annealing between pulses may result in a significantly decreased rate of damage accumulation compared to that seen under steady-state conditions. On the other hand, very high neutron fluxes in the pulse itself may severely limit recombination therefore leading to extremely fast rates of damage accumulation even at elevated temperatures.

In order to understand these effects and elucidate the role and interplay of intrinsic (material type) and extrinsic (temperature, pulse, flux, fluence) variables on damage accumulation, one needs a theoretical description that can span all relevant length and time scales. We combine MD and KMC simulations and present results of a study of damage accumulation in Cu and Fe resulting from pulsed 14 MeV neutron irradiation at pulse frequencies of 1, 10, and 100 Hz. The simulations are

carried out at a temperature just above annealing stage III where vacancies are mobile but vacancy clusters are stable. In addition, we present results for continuous irradiation at realistic fluxes for comparison to the pulsed case. The activation and binding energy values used for point defect and cluster migration and binding have been given earlier [13] and will not be discussed here.

As discussed above, each individual cascade results in a distribution of defects, some of which may be mobile depending on their properties and irradiation temperature. Because the KMC method takes into account all possible defect reactions at the correct rate depending on temperature, the simulations are ideal for evaluating the effects of pulsed irradiation on damage accumulation. After each pulse, the KMC computation allows the mobile defects to migrate and interact with other defects and traps for a time given by the pulse frequency.

The simulated dose rate corresponds to 10^{15} n/cm^2/s integrated over time. The dose rate in the pulse itself is of the order of 1.4 dpa/s in Fe, and the pulse length is 1 μs. At 4 Hz, it results in a damage rate of 150 dpa/yr. The overall conditions are intended to simulate those that would be encountered if a material were irradiated with the laser-driven 14 MeV neutron source recently proposed by Perkins et al. [15]. The recoil spectrum used corresponds to the first wall of the MFE reactor Starfire [16] and was calculated with the SPECOMP/SPECTER code [17,18].

Each microsecond pulse was simulated with 6 cascades picked at random with a probability of occurrence weighed by the modified recoil spectrum. For our KMC box of 300 nm edge length, this corresponds to instantaneous dose rates in the pulse of 1.4 dpa/s in Fe and 2.2 dpa/s in Cu.

Fig. 10(a) shows the evolution of the vacancy cluster population in Cu as a function of dose for 1, 10, and 100 Hz at a temperature of 340 K. Under these conditions, the rate of damage accumulation in Cu is not influenced by pulse frequency for frequencies above 10 Hz. However, the rate of damage accumulation decreases significantly at 1 Hz. The two controlling mechanisms of this behavior can be observed in Fig. 10(b). The sharp drop in damage in the first 0.03 s is a consequence of the rapid recombination between mobile SIA clusters and immobile vacancy clusters. It is also during this initial stage when mobile SIA loops coalesce and produce large immobile clusters. The second mechanism dominates from 0.03 s to the next pulse and is vacancy controlled. Small vacancy clusters break and free vacancies migrate and shrink sessile SIA clusters or agglomerate with other vacancy clusters, thus reducing the global cluster density. The time scale implies that at 1 Hz significant annealing can take place between pulses at this temperature, but not at 10

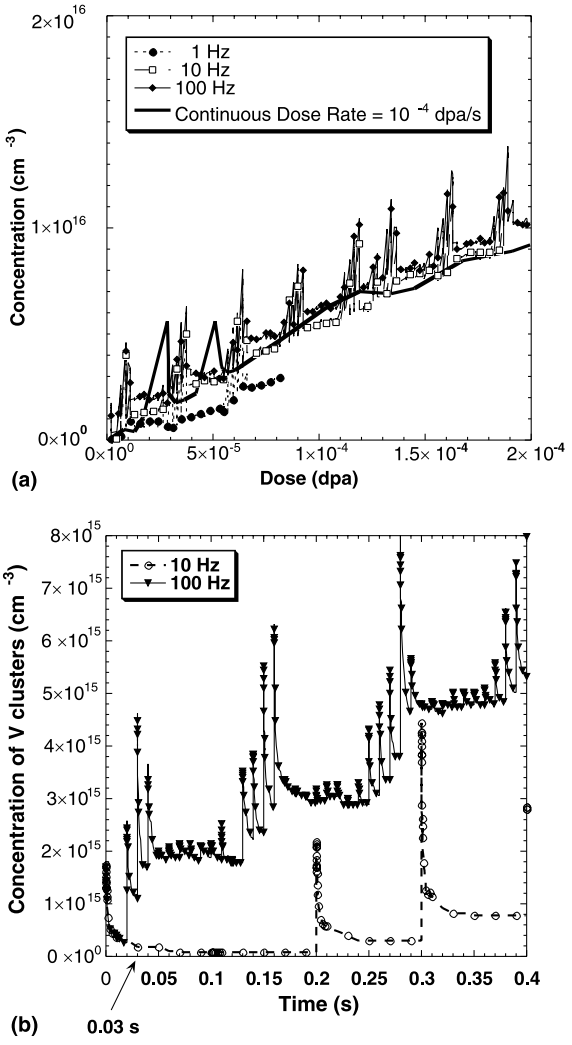

Fig. 10. Evolution of the vacancy cluster population in Cu as a function of: (a) dose at 340 K for pulse rates of 1, 10 and 100 Hz and continuous irradiation, (b) time for pulse rates of 10 and 100 Hz.

Hz or above. Continuous irradiation at 10^{-4} dpa/s results in damage densities similar to those at high pulse rates.

In Fe, the situation is somewhat different. Because bcc metals tend to contain large interstitial impurity concentrations, we carry out our simulation in the presence of 5 at. ppm impurities. These impurities are treated as traps for SIA clusters (glissile dislocation loops) with a binding energy of 1.0 eV that arises from the elastic interaction. The impurities quickly immobilize the SIA clusters, thus limiting recombination even at 1 Hz. Fig. 11(a) shows the damage accumulation in the form of vacancy clusters in Fe as a function of dose. Fig. 11(b) shows the damage production during the

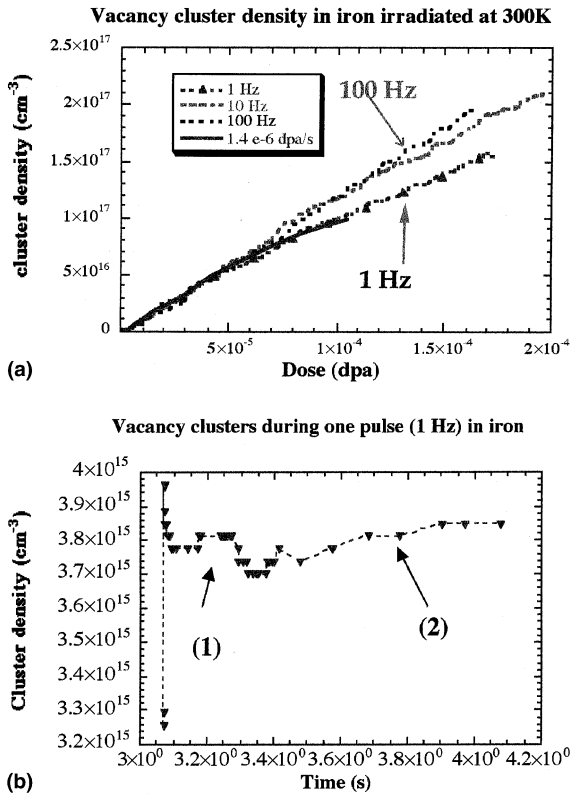

Fig. 11. (a) Evolution of the vacancy cluster density in Fe as a function of dose for pulse rates of 1, 10 and 100 Hz and continuous irradiation, (b) as a function of irradiation time for a 1 Hz pulse.

pulse and its recovery between pulses. A detailed analysis of this curve explains the damage accumulation trends in Fig. 11(a). The initial decrease in Fig. 11(b) (labeled as 1) is a consequence of vacancy recombination with fast mobile SIA clusters. Once the SIA clusters have either disappeared or been trapped by impurities, a slower process takes place. Free vacancies diffuse and either shrink interstitial clusters or agglomerate in vacancy clusters (the slope labeled as 2). This second stage takes place after 0.5 s. Therefore, the most pronounced effect in vacancy clustering is for a pulse rate of 1 Hz (Fig. 11(a)). In short, the higher the pulse rate the smaller the vacancy clusters and the higher the number of free vacancies. The pulse annealing in copper described above is slightly different. The cluster density drop in stage 1 is sharper due to the lack of impurities and the slope in stage 2 is small, due to the small number of free vacancies. A comparison of pulsed versus continuous irradiation (10^{-4} dpa/s) shows a slower damage accumulation rate under continuous irradiation. The time lapse between cascades at 10^{-4} dpa/s is 10^{-3} s, therefore vacancies do not have enough time to cluster and stay mainly as free vacancies. Lower dose rates (10^{-6} dpa/s) result in damage densities comparable to 1 Hz as shown in Fig. 11(b).

7. Conclusions

From this analysis we can conclude that the discrepancy between the experimental measurements and the calculations regarding the energy is most probably related to the values of deposited energy computed by LAHET. We have computed the correction factor to the NRT model from molecular dynamics and for the particular conditions of these experiments and found no dependence on energy or mass of the target for this factor. Since we do not expect differences in the resistivity change per Frenkel pair as a function of energy, the only possible factor that needs to be examined in more detail is the calculation of deposited energy at the high energy regime with LAHET.

We have computed the evolution of the damage at room temperature and found a large recovery of the damage due to the migration of interstitial clusters and single and small vacancy clusters to sinks such as dislocations. This large recovery has also been observed in the experiments performed by Greene et al. [11].

In addition, we have presented a study of pulsed irradiation in Cu and Fe under conditions relevant to IFE. We analyzed the influence of pulse rate and temperature in the context of defect production and clustering. In both cases we observed that the influence of pulse rate is clearly noticeable at 1 Hz, the lowest pulse rate studied, but not at higher rates. Damage recovery occurs almost instantaneously after the pulse due to fast SIA cluster migration. This recombination stage anneals out most of the damage in copper but it is rather incomplete in iron due to the presence of traps. The second annealing stage is governed by vacancies. An increase in vacancy clustering is observed in iron while the slope is flat in copper. We ascribe this difference to the high population of free vacancies in iron. It is noteworthy that at the low temperatures studied, the greatest differences in damage accumulation are between 1 and 10 Hz, which is the rate bracket where future IFE devices will operate.

Acknowledgements

Work of one of the authors (M.V.) was performed under a research grant from the Swiss National Research Fund.

References

[1] M.J. Norgett, M.T. Robinson, I.M. Torrens, Nucl. Eng. Des. 33 (1975) 50.
[2] W.J. Phythian, R.E. Stoller, A.J.E. Foreman, A.F. Calder, D.J. Bacon, J. Nucl. Mater. 223 (1995) 245.
[3] R.S. Averback, T. Diaz de la Rubia, Solid State Phys. 51 (1998).
[4] N. Soneda, T. Diaz de la Rubia, Philos. Mag. A 78 (1998) 995.
[5] S.M. Foiles, M.I. Baskes, M.S. Daw, Phys. Rev. B 33 (1986) 7983.
[6] M.W. Finnis, J.E. Sinclair, Philos. Mag. A 50 (1984) 45.
[7] J.F. Ziegler, J.P. Biersack, U. Littmark, in: J.F. Ziegler (Ed.), The Stopping and Range of Ions in Solids, vol. 1, Pergamon, New York, 1985.
[8] D.J. Bacon, F. Gao, Y.N. Osetsky, Nucl. Instrum. and Meth. B 153 (1999) 87.
[9] Y.N. Osetsky, D.J. Bacon, A. Serra, B.N. Singh, S.I. Golubov, J. Nucl. Mater. 276 (2000) 65.
[10] R. Stoller, L.R. Greenwood, Mater. Res. Soc. Symp. Proc. 538 (1999) 203.
[11] G.A. Greene, R.K. Corzine, M.R. James, BNL-66931 Internal Report, Aug. 1999.
[12] J.W. Martin, J. Phys. F 2 (1972) 842.
[13] M.-J. Caturla, N. Soneda, E. Alonso, B. Wirth, T. Diaz de la Rubia, J.M. Perlado, J. Nucl. Mater. 276 (2000) 15.
[14] M. Victoria, N. Baluc, C. Bailat, Y. Dai, M.I. Luppo, R. Schaublin, B.N. Singh, J. Nucl. Mater. 276 (2000) 114.
[15] L.J. Perkins et al., Nucl. Fus., to be published.
[16] Argonne National Laboratory, McDonnell Douglas Astronautics Co., General Atomic Co., Ralph M. Parsons Co., STARFIRE: A Commercial Tokamak fusion power study, Argonne National Lab, Argonne, IL, ANL/FPP-80-1, 1980.
[17] L.R. Greenwood, SPECOMP calculations of radiation damage in compounds, ASTM-STP 1001 (1989) 598.
[18] L.R. Greenwood, R.K. Smither, SPECTER: Neutron damage calculations for materials irradiations, ANL/FPP-TM-197, 1985.